Cement & Concrete Composites 31 (2009) 22–28

Contents lists available at ScienceDirect

Cement & Concrete Composites

journal homepage: www.elsevier.com/locate/cemconcomp

Effects of calcining conditions on the microstructure of sugar cane waste ashes (SCWA): Influence in the pozzolanic activation

E.V. Morales [a], E. Villar-Cociña [a,*], M. Frías [b], S.F. Santos [c], H. Savastano Jr. [c]

[a] Department of Physics, Central University of Las Villas, Santa Clara, Villaclara 54830, Cuba
[b] Eduardo Torroja Institute (CSIC), cl Serrano Galvache 4, 28033, Spain
[c] Faculty of Animal Science and Food Engineering, University of Sao Paulo, Rural Construction, P.O. Box 23, Pirassununga SP 13635-900, Brazil

ARTICLE INFO

Article history:
Received 1 April 2008
Received in revised form 29 October 2008
Accepted 31 October 2008
Available online 13 November 2008

Keywords:
Sugar cane ashes
Calcining temperature
Morphology
Pozzolanic activity
Kinetics
Modeling and TEM

ABSTRACT

In this paper a study of calcining conditions on the microstructural features of sugar cane waste ash (SCWA) is carried out. For this purpose, some microparticles (<90 μm) of sugar cane straw ash and sugar cane bagasse ash of samples calcined at 800 °C and 1000 are studied by combining the bright field and the dark field images with the electron diffraction patterns in the transmission electron microscopy (TEM). It is appreciated that the morphology and texture of these microparticles change when silicon or calcium are present. Furthermore, it is observed that iron oxide (magnetite Fe_3O_4) is located in the calcium-rich particles.

The microstructural information is correlated with the results of a kinetic–diffusive model that allows the computing of the kinetic parameters of the pozzolanic reaction (mainly the reaction rate constant). The results show that the sugar cane wastes ash calcined at 800 and 1000 °C have properties indicative of high pozzolanic activity. The X-ray diffraction patterns, the TEM images and the pozzolanic activity tests show the influence of different factors on the activation of these ashes.

1. Introduction

In recent years, the use of solid waste derived from agriculture as pozzolans in the manufacture of blended mortars and concrete has been the focus of new research [1–10].

In fact, the addition to concrete of ashes from combustion of agricultural solid waste is at present a frequent practice, particularly in developing countries, because of the pozzolanic activity of the ashes with lime.

It is well accepted [5–8] that the wastes of sugar cane (sugar cane straw and sugar cane bagasse) have a suitable pozzolanic activity when they are calcined at temperatures above 600 °C. The pozzolanic activity of these ashes depends on some parameters such as: the particle size, the calcining temperature, amorphous/crystalline nature and the chemical composition [1,5,9–11]. At the present time, the lime (or cement)–pozzolan reaction is not very well understood as a result of the numerous mechanisms of the pozzolan/CH interactions. Determination of the pozzolanic activity with certainty is a complex problem and so further study of the pozzolanic reaction kinetics is of both scientific interest and technological importance. Some models have been published [12] in order to study the kinetics of the pozzolanic reaction and thus characterize qualitatively and quantitatively the degree of activity of these ashes.

It is known that decreasing the pozzolan particle size and increasing the amount of amorphous silica in the above mentioned wastes can greatly improve the pozzolanic activity of the ashes [13]. All the results obtained by different methods for characterizing the pozzolanic reaction kinetics in the pozzolan–lime mixtures give a global evaluation of the effectiveness of these ashes as active additions for the cement industry. However, research works that study the agricultural waste ashes in the micro and nano-scale so as to support the explanation of their macroscopic behavior are scarce. Some research works have been reported for the case of rice husk ash [9,14,15]. For sugar cane waste ashes, these studies have not been encountered in the literature. There is little experimental evidence on the influence of the morphology of the ash particles in the calcination process and in the milling process to obtain the selected sizes (<90 μm). The advantages offered by the TEM (both bright field and dark field images) for this purpose are very well known [16,17]. An adequate evaluation of any material by TEM should consider a combination of images of bright field, diffraction and dark field.

On the other hand, an analysis of the chemical composition of the individual particles of the ashes and its relationship with the kinetic parameters determined by the traditional methods was not found in the literature.

* Corresponding author.
E-mail address: evillar@uclv.edu.cu (E. Villar-Cociña).

0958-9465/$ - see front matter © 2008 Elsevier Ltd. All rights reserved.
doi:10.1016/j.cemconcomp.2008.10.004

In this work, a preliminary study of the morphological and composition changes of the individual particles corresponding to the sugar cane bagasse and straw ashes calcined at 800 °C and 1000 °C is carried out. The microstructural information is correlated with the results of a kinetic–diffusive model that considers the elementary mechanisms of the pozzolanic reaction and allows the computation of the kinetic parameters.

2. Materials and methods

2.1. Materials

The materials analyzed were the sugar cane straw ash (SCSA) and the sugar cane bagasse ash (SCBA) calcined at 800 °C and 1000 °C in an electric furnace controlled at ±5 °C for 20 min. Once calcined, the ashes were ground and sieved to <90 μm, a fineness similar to that showed by ordinary Portland cement (OPC). Table 1 shows the designations and the chemical compositions of both SCSA and SCBA ashes calcined at 800 °C and 1000 °C, which were determined by the X-ray fluorescence technique (XRF) (model EXTRA II, Tube target: Mo, KV:50). According to Table 1, the main oxides present in ashes are SiO_2, followed by CaO. Other oxides such as Al_2O_3, Fe_2O_3, P_2O_5 and K_2O are present in smaller amounts.

2.2. Methods

2.2.1. Instrumental techniques

Mineralogical composition was studied by X-ray diffraction (Philips model PW-1700 with an X-ray tube containing a copper anode).

The characterization in the micro-scale of the ashes was carried out with a transmission electron microscope (Philips CM 120 operated at 120 KV). The bright and dark field images of the 20 particles of both ashes, jointly with the microanalysis by XEDS spectra and the electron diffraction of selected area in these particles, allowed differentiating their textures and chemical compositions.

The samples of ashes for the TEM analysis are prepared mixing 1 g of ash in 10 ml of acetone in an ultrasonic stirrer, and after this a drop of the solution was deposited in suspension on a Cu grid. The grid with the stuck particles was placed in a vacuum camera before it was placed directly in the TEM.

In order to collect the characteristic X-rays in the TEM, the samples were tilted 17°, and the beam of electrons over the sample was approximately 20 nm in diameter (a diameter much smaller than the analyzed particle) to obtain the composition in the region where the beam was placed. The time of gathering of the radiation was 100 s for all the registers.

2.2.2. Pozzolanic activity method

To carry out qualitative or quantitative determinations of the pozzolanic activity, many experimental methodologies have been developed. Most of them are based on the measurement of the reaction of pozzolanic materials with the calcium hydroxide released during cement hydration. In this work, an accelerated method was used in order to study the pozzolanic activity of these materials [18].

The test consisted of putting the pozzolanic material (1 g) in contact with a saturated calcium hydroxide (CH) solution (75 ml) in individual double cap polyethylene flasks of 100 ml capacity and maintained in an oven at 40 ± 1 °C for 1 day, 7 days, 28 days and 90 days (two flasks per period). At the end of each period, the solution was filtered and the chemical determination of CaO in the remaining solution was quantified. The fixed lime (mmol/l) was obtained by the difference between the concentration in the saturated lime solution and the CaO found in the solution in contact with the sample, at the end of a given period.

2.2.3. Mathematical model used

A kinetic–diffusive model [19] is used to describe this pozzolanic reaction in a pozzolan/lime solution system. The model is

$$\zeta o = \frac{C_0 - C_t}{C_0} = 1 - \frac{0.23 \cdot \exp\left(\frac{-3t}{\tau}\right) \cdot \left(-1 + \exp\left(\frac{t}{\tau}\right)\right) \cdot \frac{1}{\tau}}{C_0 D_e r_s} + \frac{0.23 \cdot \exp\left(-\frac{t}{\tau}\right) \cdot \frac{1}{\tau}}{C_0 K r_s^2} - C_{corr} \quad (1)$$

where D_e is the effective diffusion coefficient, K is the reaction rate constant, C_0 is the initial concentration of CH in the solution and τ is a time constant (the time interval during which the pozzolan radius diminishes until a 37% of its initial radio r_s).

The dimensionless magnitude $\xi = (C_0 - C_t)/C_0$ represents the relative loss of CH concentration and C_t represents the absolute loss of CH concentration with time for the pozzolan/lime system. The C_{corr} is a correction parameter that takes into account the concentration remainder of CH that is not consumed in the reaction. In some systems the CH is not totally consumed.

It is known that the pozzolanic reaction develops by stages. The resistances of these stages are usually very different and the stages presenting the greatest resistances (i.e. the stages that lapses more slowly) control the process. Accordingly, it is possible in certain cases to have different behavior: diffusive (described by the first term of Eq. (1)), kinetic (second term) and kinetic–diffusive (both terms). Further explanations about the model can be found in Refs. [12,19].

3. Results and discussion

3.1. Studies by XRD and TEM

Figs. 1a and 1b show the XRD patterns for the ashes calcined at 800 °C and 1000 °C, respectively. The SCSA samples show a very low crystallinity. A wide band is observed between 15° and 35° (2-theta) for both ashes, which implies the presence of vitreous matter.

Table 1
Chemical compositions of the ashes calcined at 800 °C and 1000 °C.

Samples[a]	Oxide (%)										
	SiO_2	Al_2O_3	Fe_2O_3	CaO	MgO	SO_3	K_2O	Na_2O	TiO_2	P_2O_5	LOI
SCSA1	70.20	1.93	2.09	12.20	1.95	4.10	3.05	0.50	0.02	1.40	1.81
SCSA2	70.99	2.08	2.25	12.44	2.01	4.35	3.10	0.56	0.02	1.47	0.52
SCBA1	58.61	7.32	9.45	12.56	2.04	0.53	3.22	0.92	0.34	2.09	2.73
SCBA2	59.35	7.55	9.83	12.89	2.10	0.72	3.41	0.96	0.37	2.15	0.81

[a] SCSA1: sugar cane straw ash calcined at 800 °C; SCSA2: sugar cane straw ash calcined at 1000 °C; SCBA1: sugar cane bagasse ash calcined at 800 °C; SCBA2: sugar cane bagasse ash calcined at 1000 °C.

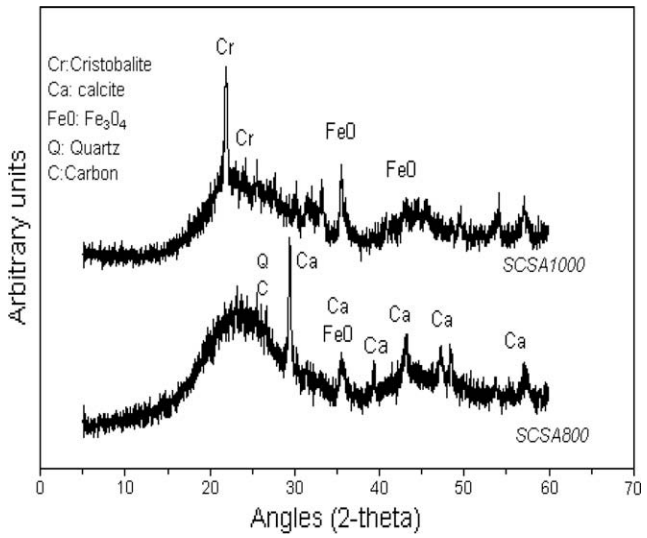

Fig. 1a. XRD corresponding to the SCSA calcined at 800 °C and 1000 °C.

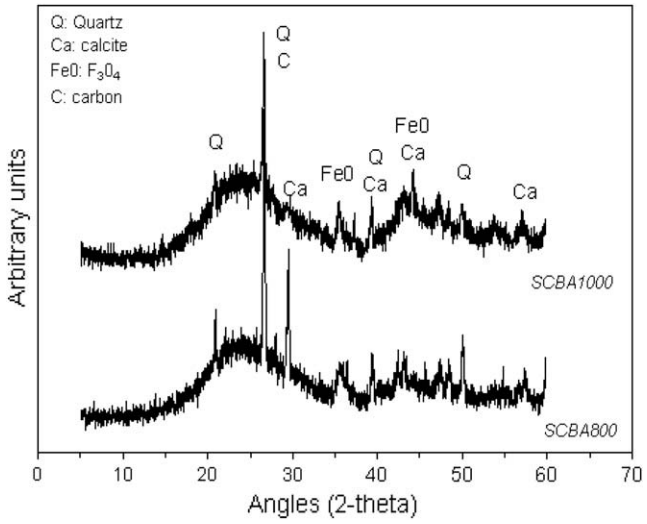

Fig. 1b. XRD corresponding to the SCBA calcined at 800 °C and 1000 °C.

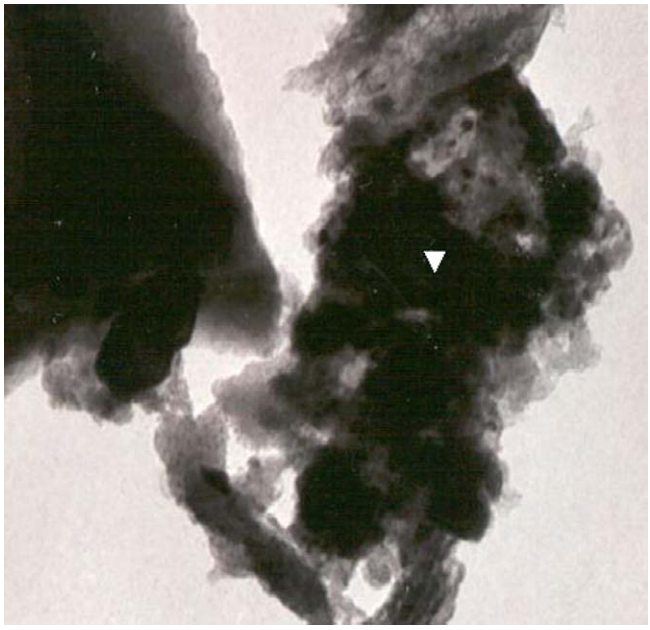

Fig. 2a. Bright field of the SCBA2 enriched in calcium oxides.

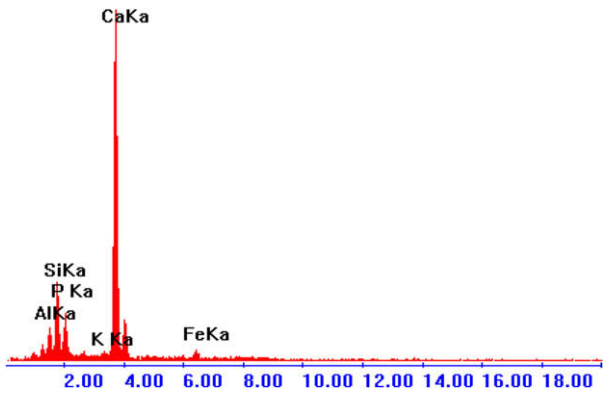

Fig. 2b. XEDS spectrum of the particle in Fig. 2a.

For SCSA1 sample, the XRD patterns suggest the presence of calcite as the main crystalline compounds, while the XRD patterns for SCSA2 suggest the alpha cristobalite as the main crystalline compounds. These results show bigger content of vitreous phase in the SCSA1 with respect to the SCSA2 given that its amounts of SiO_2 in both ashes are similar (see Table 1). This shows the direct influence of the calcining temperature on the mineralogical composition of the ashes [5] and it could be related with a recrystallization of the vitreous phase of the SiO_2 with the increase of the calcining temperature [20–22]. Other minor compounds such as iron oxides, quartz and carbon are also present. For SCBA samples (Fig. 1b), quartz is detected as the main crystalline compound and no significant differences can be detected in the vitreous and crystalline phase fractions for both calcining temperatures.

Figs. 2a and 3a show the bright field images of two different particles selected in the SCBA2, where a difference of the particle morphology can be seen. Thus, the particles in Fig. 2a are composed by a conglomerate of discontinuous and small structures and no porous texture is detected. The XEDS spectrum obtained in such conglomerate (see the arrow in Fig. 2a) showed the prevalence of Ca and not of silicon as it can be appreciated in Fig. 2b. Another type of more uniform particles with a porous texture is shown in Fig. 3a; the XEDS spectrum of these particles turned out to be very rich in Si oxides and not so rich in Ca oxides, Fig. 3b.

Similar characteristics appear in the analyzed areas of the bagasse ash particles calcined at 800 °C (SCBA1), although it was very typical to find particles with intermediate morphologies whose XEDS spectrum showed prevalence of both calcium and silicon oxides, Figs. 4a and 4b.

The TEM analyses of the SCSA samples calcined up to the given temperatures showed a similar tendency to the SCBA samples, with a slight change in the morphologies.

The conglomerates of particles rich in calcium (see arrow in Fig. 5a) were more uniform in their textures. Figs. 5a and 5b show a SCSA particle calcined at 800 °C with the features mentioned.

The electron diffraction patterns of the selected area did not detect crystals of the silicon oxides in the alpha quartz modification or cristobalite giving a typical diffuse spectrum of amorphous phases. Only those sugar cane straw and bagasse ash particles rich in Ca have a pattern as it is shown in Fig. 6, where the iron oxide Fe_3O_4 (magnetite) is well detected. These iron oxides are not detected in the electron diffraction patterns of the selected area

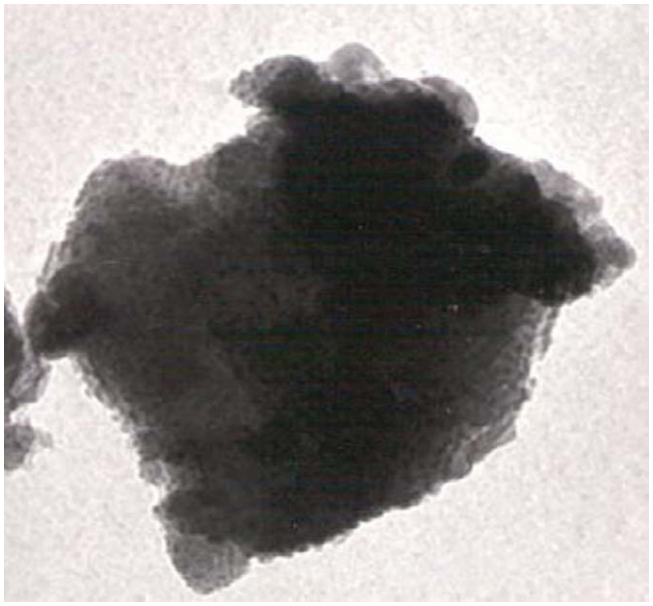

Fig. 3a. Bright field of the SCBA2 enriched in silicon oxides.

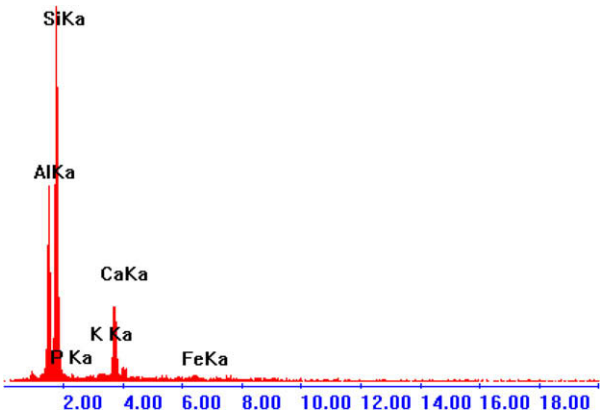

Fig. 3b. XEDS spectrum of the particle in Fig. 3a.

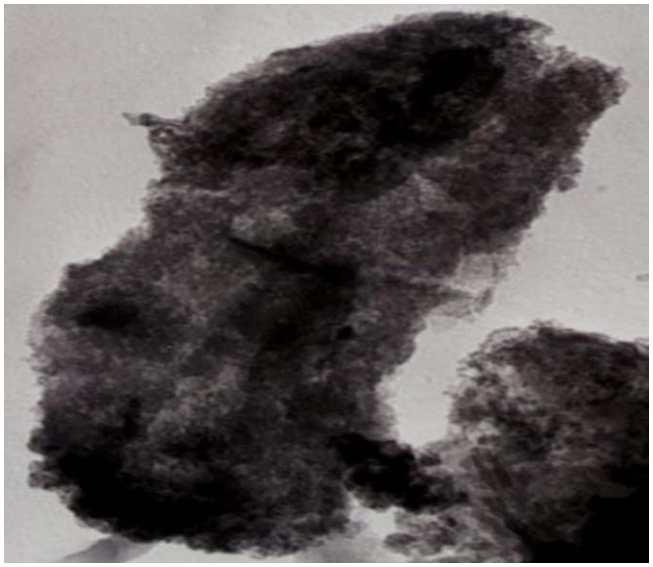

Fig. 4a. Bright field of the SCBA1, containing Si and Ca.

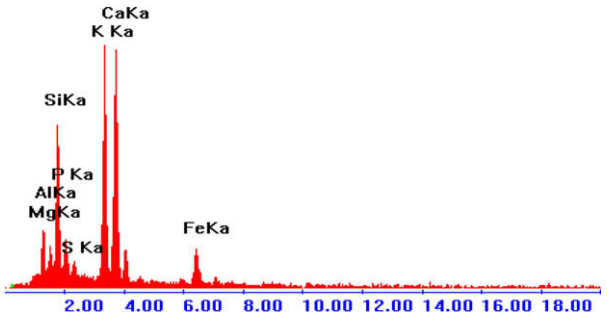

Fig. 4b. XEDS spectrum of the particle shown in Fig. 4a.

Fig. 5a. Bright field of the SCBA1, enriched in Ca.

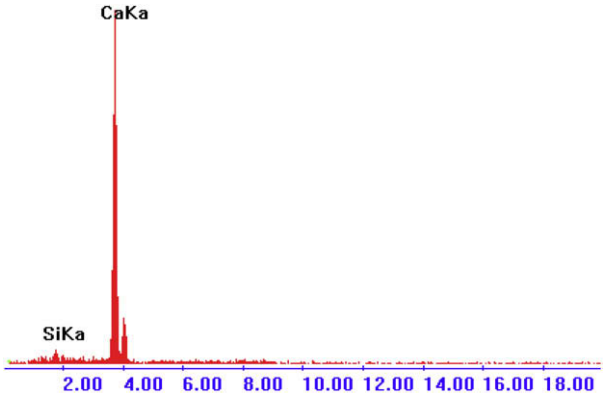

Fig. 5b. XEDS spectrum of the particle in Fig. 5a.

corresponding to those particles rich in silicon. Fig. 7 shows the non-homogeneity of the iron oxide (Fe_3O_4) distribution in the dark field image corresponding to the reflection (3 1 1) of this oxide in a SCSA particle calcined at 800 °C.

An interesting detail is that the XEDS spectra show very little Fe (Figs. 2b and 3b), while the diffraction diagrams reveal this

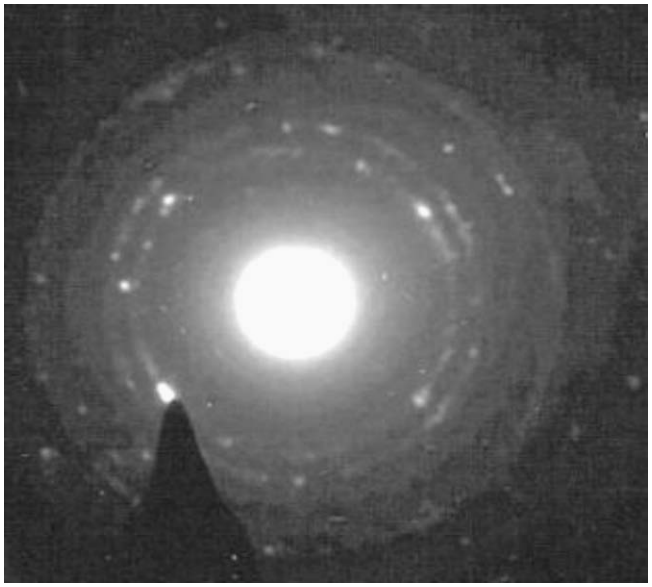

Fig. 6. Electron diffraction pattern corresponding to the Fe_3O_4.

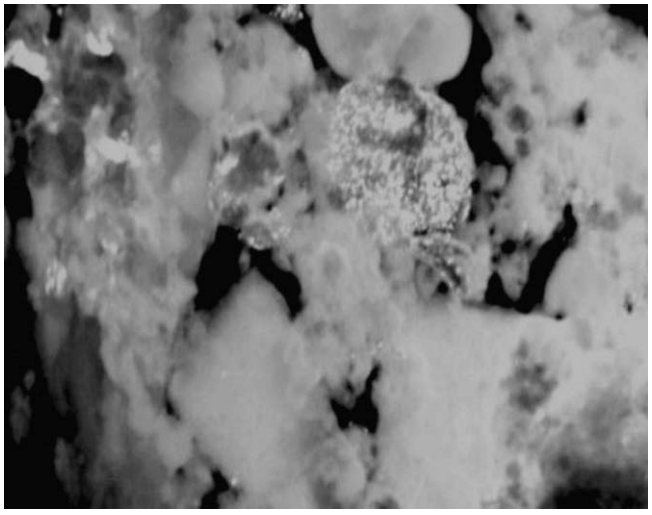

Fig. 7. Dark field image of the iron oxide (Fe_3O_4) in a SCSA1 particle.

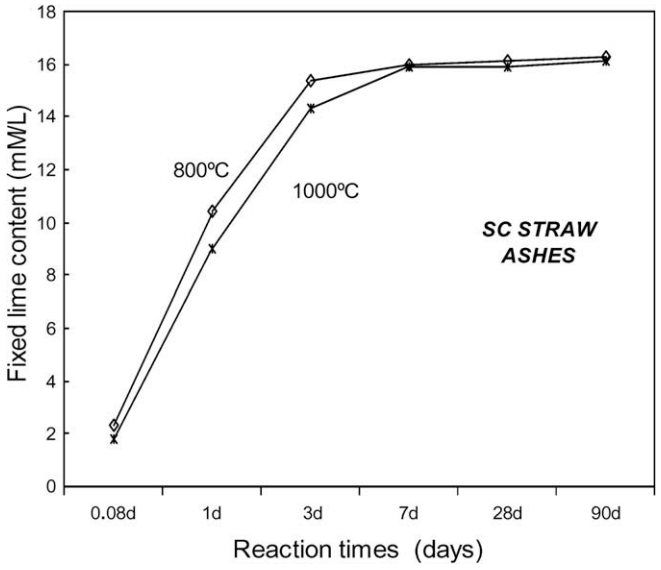

Fig. 8a. Pozzolanic activity for SCSA samples (fixed CaO content over time).

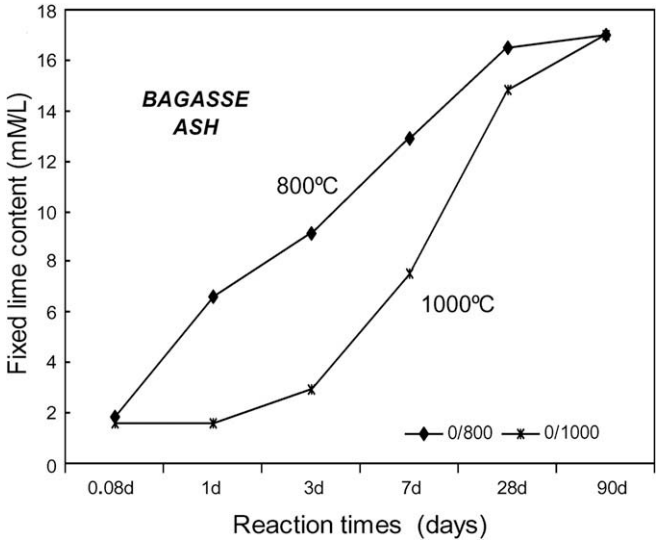

Fig. 8b. Pozzolanic activity for SCBA waste samples (fixed CaO content over time).

iron oxide with great prevalence in those particles richer in calcium oxides. This may be due to the smallness of the area scanned by the XEDS analysis with regard to a much bigger area included in the electron diffraction patterns, which indicates the non-homogeneity in the distribution of this iron oxide in the ash particles.

3.2. Pozzolanic activity and kinetic parameters

Figs. 8a and 8b show the results of the pozzolanic activity test of the studied ashes. In these, the fixed lime content (mmol/l) versus the time of reaction in days is represented. It is pointed out that the SCSA (Fig. 8a) consumes a bigger quantity of CH during the first seven days; and the experimental significance showed a slightly more intense activity for SCSA1 at 800 °C than SCSA2 at 1000 °C. The pozzolanic activity behaviors for SCBA1 and SCBA2 showed significant differences in the first seven days of curing as shown in Fig. 8b.

The kinetic–diffusive model (Eq. (1)) was applied to all samples by using non-linear regression techniques. Figs. 9a, 9b, 10a and 10b illustrate the relative loss of CH concentration versus reaction time for the SCSA/CH and SCBA/CH samples. The solid line represents the curve of the fitted model.

Fitting the relative loss of CH concentration versus time successively to the kinetic control model, diffusive control model and a mixed (kinetic–diffusive) control model and carrying out an exhaustive analysis [23–25] of the important statistical parameters such as correlation coefficient (r), coefficient of multiple determination (R^2), 95% confidence intervals, residual scatter, residual probability and variance analysis (which constitutes a rigorous evaluation of the fitting process of the model to the experimental data), allows one to conclude that the kinetic control regime predominates showing the best correspondence with the experimental data.

This means that the chemical interaction speed on the surface of the nucleus of the pozzolan particle is slower than the diffusion

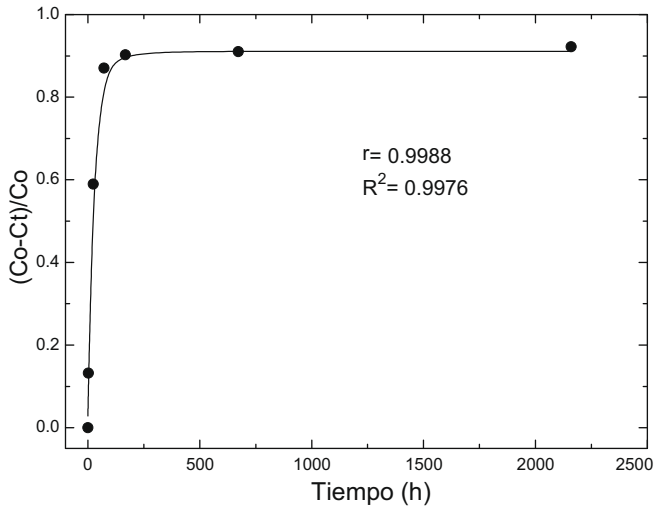

Fig. 9a. Relative loss of lime concentration plotted against reaction time for SCSA1 calcined at 800 °C. Black circle, experimental; solid line, model.

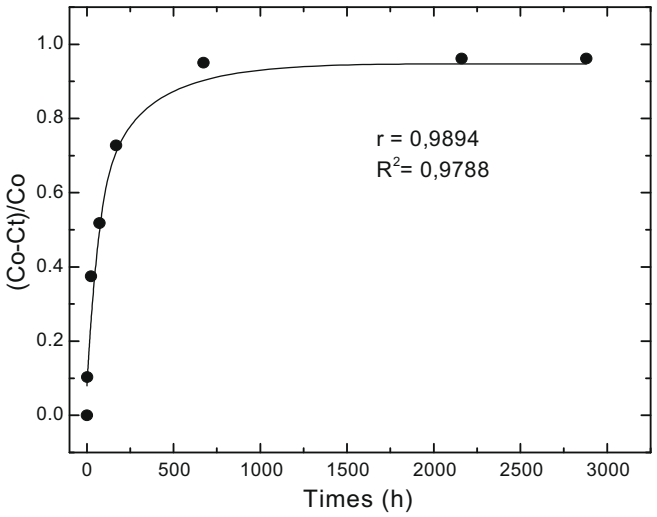

Fig. 10a. Relative loss of lime concentration plotted against reaction time for SCBA1 calcined at 800 °C. Black circle, experimental; solid line, model.

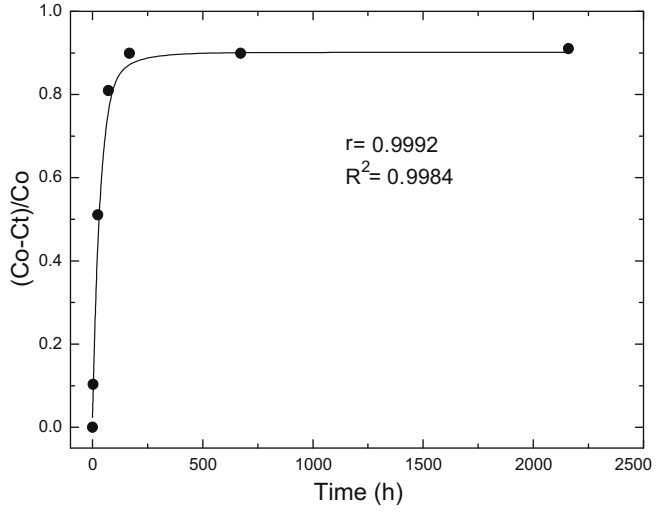

Fig. 9b. Relative loss of lime concentration plotted against reaction time for SCSA2 calcined at 1000 °C. Black circle, experimental; solid line, model.

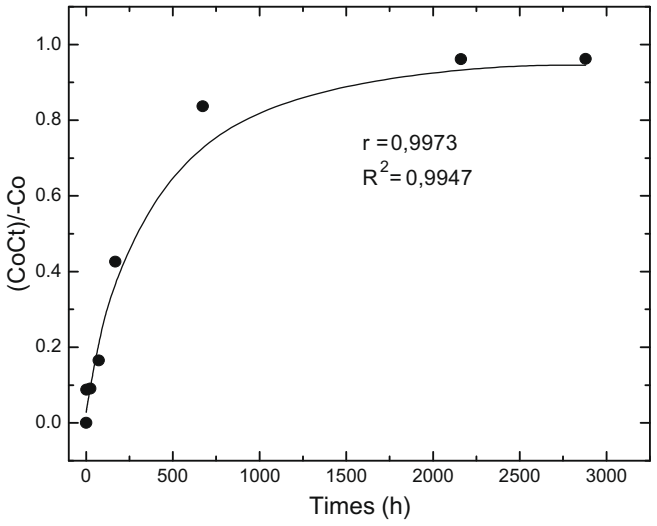

Fig. 10b. Relative loss of lime concentration plotted against reaction time for SCBA2 calcined at 1000 °C. Black circle, experimental; solid line, model.

speed of the reactant through the reaction product layer formed around the nucleus. This might be due to high porosity of the reaction product layer in these ashes, which facilitates a quick diffusion process.

In this paper, only a few statistical parameters are shown (r, R^2, SE, RSS) since the rest (mentioned above) are related to the graphic analysis and require large tables better suited for a much larger paper.

The values of the τ parameter and the reaction rate constant K are given in Table 2, whereas the correlation and multiple determination coefficients r and R^2 are shown in Figs. 9 and 10.

According to the values of the reaction rate constant K, SCSA1 shows the highest reactivity (larger value of K) followed by SCSA2, SCBA1 and SCBA2.

Traditionally, the pozzolanic reactivity is strongly related to the amorphous character of the pozzolan particle. However, the previous results shown in Section 3.1 indicate that there are other factors besides the amorphous or crystalline character of the pozzolans that have a direct incidence on their reactivity. In this sense, the analyzed SCSA showed significant differences in their contents of vitreous phases at the two calcining temperatures (see the XRD patterns), however; there was not a significant difference in their reactivities (the reaction rate constants are in the same order, Table 2). On the other hand the XRD patterns of the SCBA did not show differences of the vitreous or crystalline phase fractions corresponding to the SiO_2 oxide, while their pozzolanic reactivity showed appreciable changes, mainly in the first ages (Fig. 8b and the reaction rate constants are the different orders, Table 2).

We highlight the possible role of the porous character of the initial pozzolan particles found in the ashes and evidenced by the TEM images. So, highly porous pozzolans could also originate highly porous layers of the reaction products. This facilitates higher speed in the diffusive stage and as a consequence the chemical reaction on the surface of the unreacting pozzolan nucleus will be the controlling stage.

We assume that in the whole group of analyzed particles, the crystalline character of the SiO_2 is not detected in the electron diffraction patterns, perhaps because of the small number of samples used.

Table 2
Kinetic and statistical parameters applying the kinetic–diffusive model to the studied ashes.

Sample (ash)	τ (h)	Reaction rate constant (h^{-1})	C_{corr}	Correlation coefficient (r)	Coefficient multiple determination (R^2)	RSS
SCSA1	23 ± 2	(8.1 ± 0.7) 10^{-2}	0.08 ± 0.01	0.9988	0.9976	0.0022
SCSA2	30 ± 2	(6.3 ± 0.4) 10^{-2}	0.09 ± 0.01	0.9992	0.9984	0.0015
SCBA1	100 ± 10	(1.9 ± 0.4) 10^{-2}	0.05 ± 0.04	0.9894	0.9788	0.0022
SCBA2	333 ± 39	(5.4 ± 0.7) 10^{-3}	0.04 ± 0.02	0.9973	0.9946	0.0060

4. Conclusions

The main conclusions of the current research work can be expressed as follows:

1. These wastes, by their characteristics, can be transformed into supplementary cementing materials for the manufacture of cements and concretes.
2. The calcining temperature has a direct influence on the pozzolanic reactivity of wastes, mainly for the bagasse ashes.
3. The main textures and morphologies of the SCBA and the SCSA calcined at 800 °C and 1000 °C are shown. It is appreciated how the texture and morphology of these particles change in dependence of Ca or Si content. The non-homogeneous distribution of the minority oxides such as Fe_3O_4 in these particles is also shown.
4. The calcining temperature not only influences the mineralogical composition of the ashes but also in the morphology and composition of their individual particles.
5. The bright field image of a pozzolan particle rich in silicon showed its extremely porous character, which could have a direct incidence in the reaction mechanisms with the calcium hydroxide.
6. The values of the reaction rate constant, obtained in the fitting process of the kinetic–diffusive model, show that the sugar cane straw ash calcined at 800 °C and 1000 °C have high and similar pozzolanic reactivity. The SCBA has less pozzolanic activity than the SCSA, and its pozzolanic reactivity varies substantially with the calcining temperature.
7. The availability of ashes with different pozzolanic reaction rates can become an important technological advantage in the manufacture of new blended cement matrixes that include the calcined materials. The selection of one ash or another as the preferred pozzolan will depend on the characteristics needed for the building site.
8. Future studies include in depth analyses about the degree of influence of the amorphous character and other factors on the pozzolanic reactivity.

Acknowledgements

The authors thank CAPES (Brazil) for the financial support offered through the project CAPES-MES/Cuba No. 018/06. We also extend our gratefulness to the DEMA of the UFSCar (Brazil) for their support with transmission and scanning electron microscopy and Dr. M. Llanes for reading the manuscript. This work was also supported by CSIC (Spain) and CITMA (Cuba) (Research Project: 2003CU009).

References

[1] Chandrasekhar S, Pramada PN, Majeed J. Effect of calcination temperature and heating rate on the optical properties and reactivity of rice husk ash. J Mater Sci 2006. doi:10.1007/s10853-006-0859-0.
[2] de Souza C, Ghavami K, Stroeven P. Porosity and water permeability of rice husk ashblended cement composites reinforced with bamboo pulp. J Mater Sci 2006. doi:10.1007/s10853-006-0217-2.
[3] Cordeiro GC, Filho RDT, Tavares LM, Fairbairn EMR. Pozzolanic activity and filler effect of sugar cane bagasse ash in Portland cement and lime mortars. Cem Concr Compos 2008;30:410–8.
[4] Ganesan K, Rajagopal K, Thangavel K. Evaluation of bagasse ash as supplementary cementitious material. Cem Concr Compos 2007;29:515–24.
[5] Frias M, Villar-Cociña E, Valencia-Morales E. Characterisation of sugar cane straw waste as pozzolanic material for construction: calcining temperature and kinetic parameters. Waste Manage 2007;27:533–8.
[6] Villar-Cociña E, Frias Rojas M, Valencia-Morales E. Sugar cane as pozzolanic materials: application of a mathematical model. ACI Mater J 2008;105(3):258–64.
[7] Payá J, Monzó J, Borrachero MV, Díaz-Pinzón L, Ordoñez LM. Sugar-cane bagasse ash (SCBA): studies on its properties for reusing in concrete production. J Chem Technol Biotechnol 2002;77:321–5.
[8] Baguant K. Properties of concrete with bagasse ash as fine aggregate. In: Malhotra VM, editor. Proceedings of the fifth CANMET/ACI international conference on fly ash, sílica fume, slag and natural pozzolanas in concrete, Milwauke; 1995. p. 153–118.
[9] Chandrasekhar S, Satyanarayana KG, Pramada PN, Raghavan P, Gupta TH. Review processing, properties and applications of reactive silica from rice husk—an overview. J Mater Sci 2003;38:3159–68.
[10] Majumdar AJ, Larner LJ. The Measurement of pozzolanic activity. Cem Concr Res 1977;7:209–10.
[11] Sata V, Jaturapitakkul C, Kiattikomol K. Influence of pozzolan from various byproduct materials on mechanical properties of high-strength concrete. Constr Build Mater 2007;21:1589–98.
[12] Villar-Cociña E, Frias M, Valencia-Morales E, Sánchez de Rojas MI. An evaluation of different kinetic models for determining the kinetic coefficients in sugar cane straw–clay ash/lime system. Adv Cem Res 2006;18:17–26.
[13] Madruga F. Western opaline rocks of Spain. Applications with construction materials and evaluation of their pozzolanicity by conductometric techniques. In: Junta de Castilla y León, Consejería de Fomento. Valladolid; 1991. p. 94.
[14] Abreu RF, Schneider J. Structure and hydration kinetics of silica particles in rice husk ash studied by ^{29}Si high-resolution nuclear magnetic resonance. J Am Ceram Soc 2005;88:1514–20.
[15] Nair DG, Fraaij A, Klaassen AAK, Kentgens APM. A structural investigation relating to the pozzolanic activity of rice husk ashes. Cem Concr Res 2008;38:861–9.
[16] Sharma R. An environmental transmission electron microscope for in situ synthesis and characterization of nanomaterials. J Mater Res 2005;20:1695–707.
[17] Utsunomiya S, Ewing R. Application of high-angle annular dark field scanning transmission electron microscope, scanning transmission microscopy-energy dispersive X-ray spectrometry, and energy-filtered transmission electron microscopy to the characterization of nanoparticles in the environment. Environ Sci Technol 2003;37:786–91.
[18] Frias M, Villar-Cociña E, Sanchez de Rojas MI, Valencia-Morales E. The effect that different pozzolanic activity methods has on the kinetic constants of the pozzolanic reaction in sugar.... Cem Concr Res 2005;35:2137–42.
[19] Villar-Cociña E, Valencia-Morales E, Gonzalez-Rodríguez R, Hernandez-Ruíz J. Kinetics of the pozzolanic reaction between lime and sugar cane straw ash by electrical conductivity measurement: kinetic–diffusive model. Cem Concr Res 2003;33:517–24.
[20] Boateng A, Skeete D. Incineration of rice hull for use a cementitious material: the Guyana experience. Cem Concr Res 1990;20:795–802.
[21] Khangaonkar PR, Rahmat A, Jolly Kutty KG. Kinetic study of the hydrothermal reaction between lime and rice-husk-ash silica. Cem Concr Res 1992;22:577–88.
[22] Malhotra SK, Dave NG. Investigations into the effect of addition of fly ash and burnt clay pozzolana on certain engineering properties of cement composites. Cem Concr Compo 1999;21:285–91.
[23] Seber GAF, Wild CJ. Nonlinear regression. New York: Wiley & Sons; 1989.
[24] Ratkowsky DA. Nonlinear regression modelling: a unified practical approach. New York: Marcel Dekker, Inc.; 1983.
[25] Shwarz G. Estimating the dimension of a model. Ann Stat 1978;6:461–4.